Energy Research and Development Division

FINAL PROJECT REPORT

Solar-Reflective "Cool" Walls: Benefits, Technologies, and Implementation

Appendix H: Effects of Self-cleaning Walls on Urban Air Quality (Task 3.5 Report)

California Energy Commission
Gavin Newsom, Governor

April 2019 | CEC-500-2019-040-APH

Appendix H: Effects of self-cleaning walls on urban air quality (Task 3.5 report)

Jiachen Zhang[1], Yun Li[1], Hugo Destaillats[2], Xiaochen Tang[2], Ronnen Levinson[2], and George Ban-Weiss[1]

[1] Department of Civil and Environmental Engineering, University of Southern California, Los Angeles, CA, USA

[2] Lawrence Berkeley National Laboratory, Berkeley, CA, USA

28 February 2018

Abstract

We analyze total NO_x deposition in Los Angeles County assuming a hypothetical scenario where all walls are painted with photocatalytic cool paints. We use laboratory-measured dry deposition velocities for NO_x (0.2-0.5 cm s^{-1}), and wall-to-urban land area ratios derived from a real-world building dataset. Total expected deposition is compared to recent (2012) emissions of NO_x in urban Los Angeles County to assess the magnitude of predicted deposition increases.

Daytime (05:00 LST–19:00 LST) total NO_x deposition and emissions are 6.6×10^3–1.6×10^4 mol day^{-1} and 3.3×10^6 mol day^{-1}, respectively. Therefore, daytime NO_x deposition is 0.2-0.5% of NO_x emissions in July in Los Angeles County. Thus, adopting photocatalytic cool walls is expected to have small impacts on regional air quality in Los Angeles. Note that this analysis estimates city-level NO_x deposition, and does not consider whether photocatalytic self-cleaning walls may have larger air quality benefits for near-source concentrations in urban canyons (i.e., the space between buildings and above streets). We suggest future work to estimate the impact of photocatalytic walls on near-source NO_x concentrations.

1 Introduction

Photocatalytic self-cleaning cool wall products are designed to maintain high albedos in polluted environments. Use of photoactive titanium dioxide (TiO_2) pigments in surface coatings or paints enable soiling to be oxidized under sunlight and then washed away. A possible co-benefit of these photocatalytic coatings and paints is that they can remove NO_x from ambient air, and potentially influence ambient gas- and particle-phase pollutant concentrations.

Land et al. (2009) carried out experiments to measure the deposition of NO_x onto TiO_2-impregnated surfaces. Using their upper bound measured deposition velocities and assuming that all urban surfaces in the area were impregnated with photoactive TiO_2, NO_x deposition was calculated as ~1% of total NO_x emissions in Fulton County, Georgia. Note that their estimate did not take into consideration the real-world wall area in the region.

Here we present an analysis to quantify the total NO_x deposition in Los Angeles County assuming a hypothetical scenario where all walls are painted with photocatalytic cool paints. We conduct laboratory experiments to measure dry deposition velocities of NO_x and derive wall-to-urban land area ratios from a real-world building dataset. Finally, our computed total NO_x deposition in urban Los Angeles County is compared to recent emissions (i.e., for 2012) to assess the magnitude of predicted deposition increases.

2 Methods

2.1 Measuring NO_x deposition velocities to photocatalytic surfaces in the laboratory

We conducted experiments that tested the NO_x removal abilities of two photocatalytic cool wall products, as detailed in Task Report 4.3. Measured values of the NO_x deposition velocities onto photocatalytic wall materials ranged between 0.02 to 0.05 cm s^{-1}.

2.2 Analysis approach

For a first order approximation, we assume that the deposition velocity onto cool walls is constant throughout the daytime, suggesting that the flux of UV photons is not the rate limiting factor. While this is likely not true, our goal is to quantify upper bound estimates of NO_x deposition to compare with total NO_x emissions in Los Angeles County.

The hourly averaged NO_x deposition (mol hr^{-1}) D_{NO_X} in the urban areas of Los Angeles County, induced by adopting photocatalytic walls, is computed as

$$D_{NO_X} = C_{NO_X} \times V_{NO_X} \times A_{Wall} \times k \quad (1)$$

where C_{NO_X} is NO_x concentration (ppbv) (see Section 2.3.4), V_{NO_X} is the NO_x deposition velocity onto photocatalytic walls (cm s^{-1}) derived using laboratory experiments (see Section 2.1), A_{Wall} is total wall area (m^2) in Los Angeles County (see Section 2.3.2), and k is a unit conversion factor (i.e., 1.5×10^{-6} $\frac{\text{mol s}}{\text{ppbv cm m}^2\text{ hr}}$) assuming atmospheric pressure is 1.01×10^5 Pa and temperature is 298.15 K.

E_{NO_X}, the hourly averaged NO_x emissions (mol hr^{-1}) from urban areas in Los Angeles County, is computed as,

$$E_{NO_X} = F_{NO_X} \times A_{Land} \quad (2)$$

where F_{NO_X} is the emission flux (mol m^{-2} hr^{-1}) (see Section 2.3.3) and A_{Land} is total land area (m^2) in Los Angeles County (see Section 2.3.1).

2.3 Datasets used for analysis

2.3.1 Urban land area

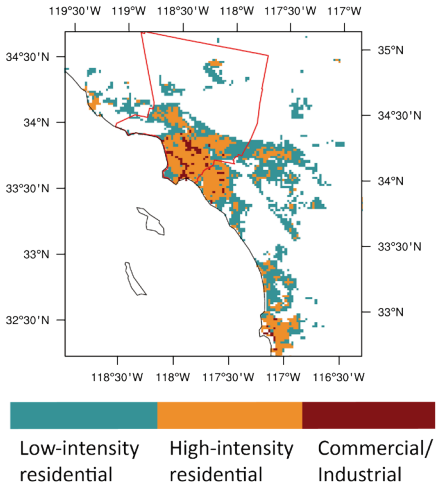

Figure 1. Map of dominant urban land use types, as defined by National Land Cover Database (NLCD). Los Angeles County is bounded by red outline.

The entire Los Angeles County (excluding Santa Catalina Island and Terminal Island) is divided into 2,650 grid cells of 2×2 km^2, where 803 grid cells are classified as urban. Figure 1 shows the land use types for urban grid cells based on National Land Cover Database (NLCD) classification. Low-intensity residential, high-intensity residential, and commercial/industrial land use types are assumed to have different urban morphological properties (e.g., roof to land area ratio and wall to land area ratio).

2.3.2 Wall to urban land area ratio

For each urban land use type, the ratio of wall area to urban land area is derived from a real-world dataset for Los Angeles County, LARIAC (2016). This dataset provides information for every building in Los Angeles County, including ZIP Code, roof area, building height, and building shape. See more details on this dataset and procedures in Section 2.3 of the Task 3.2 report: *Urban climate impacts of cool walls* (Appendix E).

2.3.3 Emission inventories

We use state-of-the-science emission inventories for 2012 from the South Coast Air Quality Management District (SCAQMD). SCAQMD provides hourly emissions for the entire year at 4-km resolution. These emissions represent all anthropogenic sources including motor vehicles, point sources such as refineries, and off-road sources. Biogenic and biomass burning emissions are not considered. The emissions data are re-gridded to 2-km resolution to match the land use classification dataset.

2.3.4 Observed NO_x concentrations

We attain NO_x concentrations for 13 monitoring stations in Los Angeles County from the Air Quality System (AQS). AQS data are collected from local, state, and federal air quality control agencies.

2.4 Caveats

The laboratory experiments reported in Task report 4.3 use a UV-A (i.e., wavelength ranging between 315-400 nm) irradiance of 11.5 W m^{-2}. In the real atmosphere, the UV intensity may differ from this laboratory UV irradiance and varies by time of day. UV irradiance may affect both hourly variation and the overall magnitude of NO_x deposition velocity. In particular, our calculations may overestimate NO_x removal during early morning and late afternoon, when UV intensity is low. For this reason, the deposition values reported here can be considered upper bounds estimates. Also note that laboratory experiments were carried out at NO_x concentrations of 300 – 1000 ppb, which is higher than typical ambient NO_x concentrations.

3 Results and discussion

3.1 The diurnal cycle NO_x concentrations

Figure 2 shows the diurnal cycle of observed NO_x concentrations. NO_x reaches its daily maximum of 26 ppbv at 06:00 LST. This can be attributed to (1) morning traffic that emits NO_x, and (2) the relatively low atmospheric boundary layer heights for early morning hours. Lower atmospheric boundary layer heights reduce the volume of air where pollutants disperse, and therefore lead to higher pollutant concentrations per emissions.

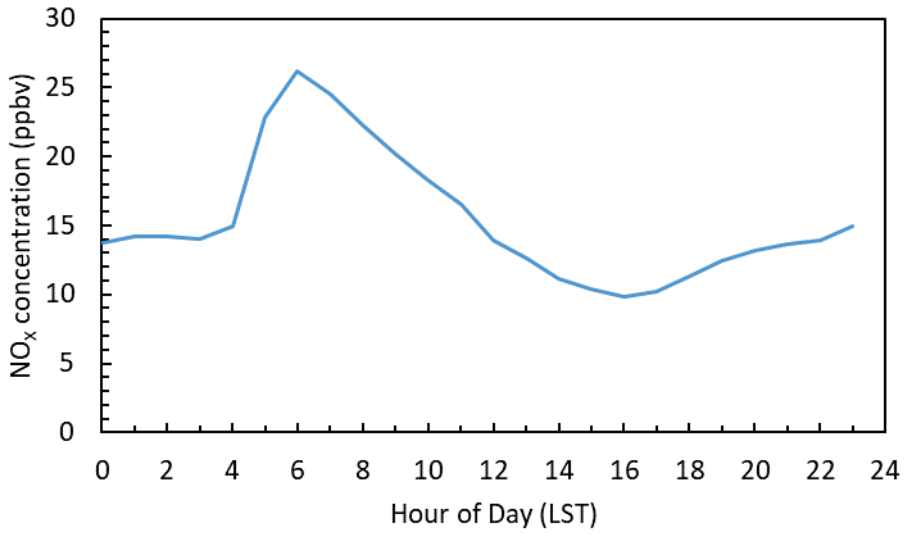

Figure 2. Diurnal cycle of observed NO_x concentrations averaged among 13 AQS sites in Los Angeles County. Each hour of day marks beginning of an hour. Values are averaged for July, 2012.

3.2 Total urban land area and wall area

Table 1 shows the urban land area and wall area for each urban land use type and other data used to compute these areas. Ratio of roof area to urban land area ($f_{R\ to\ L}$) is calculated from LARIAC (2016). Ratio of wall area (excluding windows) to roof area ($f_{W\ to\ R}$) is determined from LARIAC (2016) that provides ratio of gross wall area to roof area (detailed in Task 3.2 report) and Table 5.1 in Rosado (2016) that provides the ratio of window to wall area. Specifically, the ratio for the single-family home prototype (14.1%) is assigned to the low-intensity residential and high-intensity residential land use types, while that for retail stand-alone (7.1%) is assigned to commercial/industrial. Ratio of wall area to urban land area ($f_{W\ to\ L}$) is then calculated as $f_{R\ to\ L} \times f_{W\ to\ R}$. Total urban land area is calculated as the number of grid cells multiplied by 4 km^2. Multiplying total urban land area by $f_{W\ to\ L}$, we attain total wall area for each land use type. Total urban land area and wall area in Los Angeles County are 3,212 km^2 and 895 km^2, respectively.

Table 1. Ratios of roof to urban land area, wall to roof area, wall to urban land area, numbers of grid cells, as well as total urban area and wall area for the three NLCD urban land use types (Figure 1) in urban Los Angeles county.

Land use type	Ratio of roof area to urban land area ($f_{R\ to\ L}$)	Ratio of wall area (excluding windows) to roof area ($f_{W\ to\ R}$)	Ratio of wall area (excluding windows) to urban land area ($f_{W\ to\ L}$)	Number of grid cells	Total urban land area (km^2)	Total wall area (km^2)
Low-intensity residential	0.13	1.68	0.21	379	1,516	318
High-intensity residential	0.19	1.68	0.33	371	1,484	484
Commercial and industrial	0.23	1.95	0.44	53	212	93

3.3 NO_x deposition in July

Figure 3a shows the diurnal cycle of NO_x deposition in July. Based on the lower bound of measured NO_x dry deposition velocity (0.02 cm s^{-1}), NO_x deposition ranges from 267 – 709 mol hr^{-1}, depending on time of day. Based on the upper bound of NO_x dry deposition velocity (0.05 cm s^{-1}), NO_x deposition ranges from 668 – 1,770 mol hr^{-1}. The diurnal variability for estimated NO_x deposition follows that for ambient NO_x concentrations (see Figure 2 and Eq. 1).

(a)

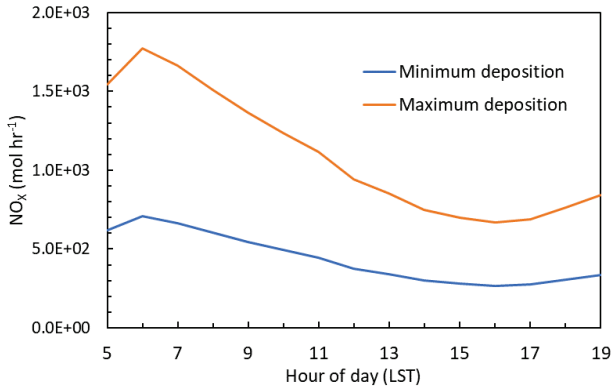

(b)

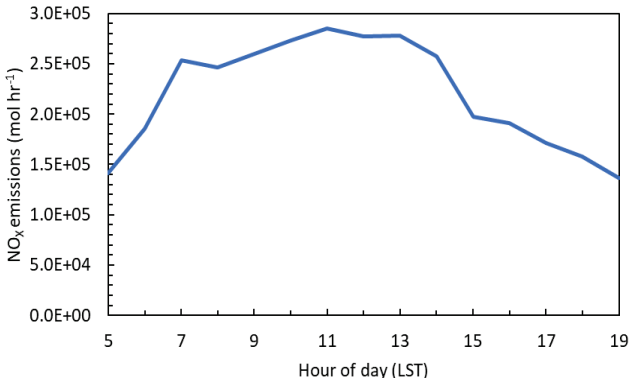

(c)

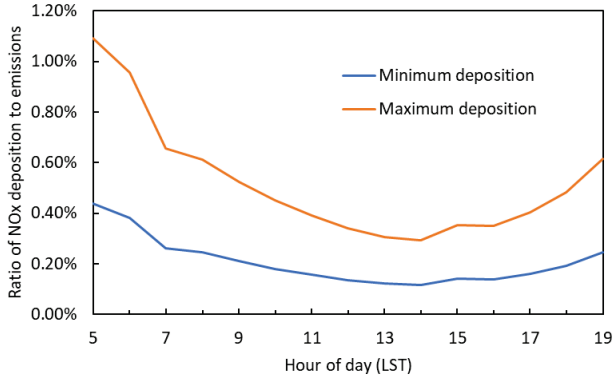

Figure 3. Diurnal cycles for urban Los Angeles County of (a) NO_x deposition (mol hr^{-1}); (b) NO_x emissions (mol hr^{-1}); and (c) the ratio of NO_x deposition to emissions. Values are averaged for July, 2012. Panels (a) and (c) show upper and lower bound estimates based on variations in measured dry deposition velocities (Section 2.1).

3.4 NO_x emissions in July

Figure 3b shows the hourly NO_x emissions during daytime averaged in July. NO_x emissions reach a maximum at 11:00 LST. NO_x emissions are in the range of $(1.3–2.8) \times 10^5$ mol hr^{-1}. The emissions start to increase with the morning traffic and peak around noon. The diurnal cycle of NO_x emissions is driven by the diurnal variations of on-road and off-road mobile sources and stationary sources (South Coast Air Quality Management District, 2013).

3.5 Discussion

Figure 3c shows the diurnal cycle of the ratio of NO_x deposition to emissions. Even when assuming the maximum deposition velocity measured in experiments, the upper bound daily maximum NO_x deposition is less than 1.1% of NO_x emissions.

Daytime (05:00 LST–19:00 LST) total NO_x deposition and emissions are 6.6×10^3–1.6×10^4 mol day^{-1} and 3.3×10^6 mol day^{-1}, respectively. Therefore, daytime NO_x deposition is 0.2-0.5% of NO_x emissions in July in LA County. Thus, adopting photocatalytic cool walls is expected to have small impacts on regional air quality in Los Angeles

This analysis estimates city-level NO_x deposition, and does not consider whether photocatalytic self-cleaning walls may have larger air quality benefits for near-source concentrations in urban canyons (i.e., the space between buildings and above streets). We suggest future work to estimate the impact of photocatalytic walls on near-source NO_x concentrations.

4 Conclusions

Using laboratory measured NO_x dry deposition velocities and wall to urban land area ratios derived from a real-world building dataset, we evaluate the total NO_x deposition from adopting photocatalytic self-cleaning cool walls in Los Angeles County. Total daytime deposition of NO_x in urban Los Angeles County for July is found to be at most 0.5% of NO_x emissions. Therefore, adopting photocatalytic cool walls is likely to have a small influence on regional air quality in Los Angeles.

References

Land, E., Bergin, M. and Huey, G.: Photocatalytic Degradation of NO_x by TOTO's Hydrotect (TiO2 Impregnated) Surfaces, 2009.
https://www.pharosproject.net/uploads/files/sources/2734/1395334647.pdf

LARIAC: Countywide Building Outlines, 2016. https://egis3.lacounty.gov/dataportal/lariac/ (Accessed 11 July 2017)

Rosado, P. J.: Evaluating Cool Impervious Surfaces: Application to an Energy-Efficient

Residential Roof and to City Pavements, University of California, Berkeley. 2016. https://escholarship.org/uc/item/6bf80485

South Coast Air Quality Management District: Air Quality Management Plan (Modeling and Attainment Demonstrations), Appendix V, 2013, http://www.aqmd.gov/docs/default-source/clean-air-plans/air-quality-management-plans/2012-air-quality-management-plan/final-2012-aqmp-(february-2013)/appendix-v-final-2012.pdf

AQS: Air Quality System, https://aqs.epa.gov/api (Accessed 30 July 2017)